Electrocatalysis (2025) 16:440–450
https://doi.org/10.1007/s12678-025-00928-8

RESEARCH

Electrochemical Detection of Miltefosine in Urine Using Amino Functionalised Multi-walled Carbon Nanotubes and $[Fe(CN)_6]^{-3/-4}$ as a Redox Couple

Darko Kwabena Adu[1] · Zondi Nate[2] · John Alake[1] · Blessing Wisdom Ike[1] · Lungelo Miya[1] · Sachin Balaso Mohite[1] · Ruchika Chauhan[1] · Rajshekhar Karpoormath[1]

Accepted: 3 January 2025 / Published online: 29 January 2025

Abstract

Miltefosine is an alkyllylosophospholipid analogue used to treat visceral leishmaniasis. Recently, reports have been made of suspected counterfeit miltefosine on the Indian market. With the risk counterfeit drugs pose to drug resistance development, quality control of antileishmanial drugs has become important. Hence, in this study, amino-functionalized multi-walled carbon nanotubes (MWCNT-NH_2) were synthesised and characterised using Fourier transform infrared spectroscopy, scanning electron microscopy, and energy-dispersive X-ray spectroscopy. Also, electrochemical impedance spectroscopy and cyclic voltammetry were used to study the electrochemical properties of the synthesised MWCNT-NH_2. A complex was formed between MWCNT-NH_2 and miltefosine (Mil-MWCNT-NH_2). Five microliters of Mil-MWCNT-NH_2 was drop-cast on glassy carbon electrode, and differential pulse voltammetry studies were carried out to assess the performance of the sensor. Using $[Fe(CN)_6]^{-3/-4}$ as a redox couple, a calibration study was carried out at different concentrations (0–250 µM) to establish the concentration range of the sensor. A linear response was established. With a detection limit of 1 µM, the fabricated sensor is a viable tool for detecting antileishmanial drug miltefosine in urine samples and possible application in quality control of miltefosine against counterfeiting.

✉ Rajshekhar Karpoormath
karpoormath@ukzn.ac.za

[1] Department of Pharmaceutical Chemistry, College of Health Sciences, University of KwaZulu-Natal, Westville-Campus, 4000 Durban, South Africa

[2] Chemistry Department, Faculty of Applied Sciences, Cape Peninsula University of Technology, 7530 Bellville, South Africa

Graphical Abstract

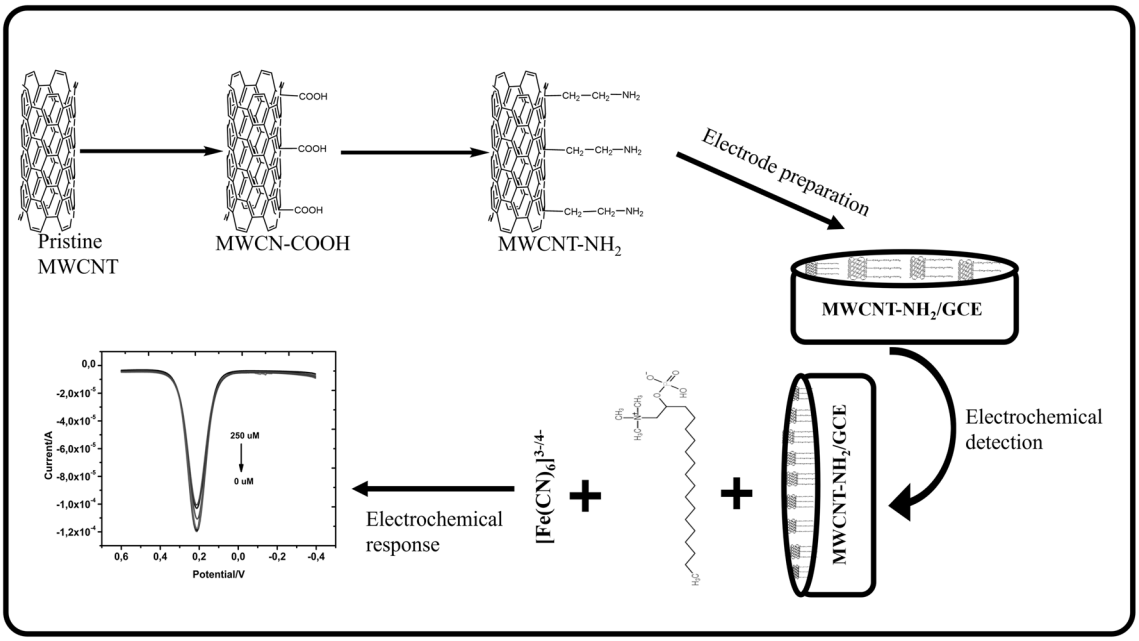

Keywords Miltefosine · Differential pulse voltammetry · Redox couple · Amino-functionalised multi-walled carbon nanotubes · Visceral leishmaniasis

Background

Leishmaniasis is a spectrum of neglected tropical diseases caused by a group of *Leishmania* parasites. Cutaneous leishmaniasis, mucocutaneous leishmaniasis, and visceral leishmaniasis are the three forms of leishmaniasis [1, 2]. Visceral leishmaniasis, the dreadful form of leishmaniasis caused by *Leishmania donovani* complex, is fatal if left untreated [3]. The disease mainly affects the poorest people in developing countries. To date, chemotherapy remains the only alternative for treating leishmaniasis [4]. Amphotericin B, miltefosine, paromomycin, and pentavalent antimonials are the few available drugs for treating the disease [5]. The financial difficulties prevalent in the leishmaniasis endemic regions create a fertile environment for counterfeiting drugs. Counterfeit drugs, which contain little or no active compound, not only present a risk to the health of patients but also adversely threaten attempts made towards control of infectious diseases and contribute to the development of drug resistance [6]. Developing an affordable and simple method to evaluate the quality of drugs used in resource-poor countries is therefore important.

Recently, reports have been made about suspected counterfeits of miltefosine in the Indian market [6]. Miltefosine is an alkyllylosophospholipid analogue used to treat visceral leishmaniasis [7, 8]. Originally, miltefosine was designed for the treatment of breast cancer and other solid tumours, which failed because of dose-limiting gastrointestinal toxicity when taken orally [8]. Miltefosine has been added to the World Health Organisation's list of essential drugs since 2010. Currently, miltefosine is the foremost and only available effective oral drug for treating leishmaniasis [9]. This underscores the importance and the need to develop quality control methods to safeguard the drug from developing resistance. In the past, analytical methods such as near-infrared spectrophotometry, liquid chromatography tandem mass spectrometry, and Fourier-transform infrared spectrophotometry have been employed to detect miltefosine [6]. However, these techniques are expensive, require multiple steps, and require skilled personnel. Surprisingly, electrochemical sensors, which are affordable, handy, selective, sensitive, and simple, have not been considered.

Electrochemical sensors are analytical devices which convert electrochemical information into beneficial signals [10]. An electrochemical sensor is made of a chemical recognition system and physicochemical transducer. The chemical recognition system is an important part of an electrochemical sensor whose role is to identify or interact with the chemical analyte [11]. On the other hand, the physicochemical transducer component transforms chemical responses into signals that electrical instrumentation can detect [12]. The two components form the working electrode, which,

together with the reference electrode and the counter electrode, form the electrochemical unit for measurements [13]. To establish an enhanced performance of electrochemical sensors, the surface of the working electrode is modified with electrocatalytic materials. Electrocatalytic materials such as conducting polymers, carbon-based materials, metal oxides, and metal–organic frameworks are used to modify the surface of the electrodes to improve conductivity and selectivity towards analytical targets [14]. Carbon nanotubes can enhance electron transfer rate, improve conductivity, and provide a large surface area [15, 16]. Aside from the positives of carbon nanotubes, the lack of functional groups on the surface affects their solubility, which makes working with carbon nanotubes challenging. To address this challenge, functional groups such as carboxyl, hydroxyl, and amine groups are attached to the surface of carbon nanotubes to improve the solubility of carbon nanotubes [17].

Based on this, this study seeks to develop a novel amino functionalised multi-walled carbon nanotube-based electrochemical sensor to detect miltefosine. Multi-walled carbon nanotubes were functionalised with amino groups to improve solubility. Also, the attachment of the amino groups facilitated the formation of a complex between the multi-walled carbon nanotubes and the miltefosine via hydrogen bonding. Miltefosine has no electroactive centre; hence, $[Fe(CN)_6]^{-3/-4}$ was used as a redox couple. Moreover, the study employed Fourier transform infrared spectroscopy, scanning electron microscopy, transmission electron microscopy, energy dispersive x-ray spectroscopy, and electrochemical technique to characterise the fabricated amino functionalised multi-walled carbon nanotubes. Finally, the study involved the detection of miltefosine in spiked urine samples.

Methodology

Materials

Potassium chloride (Merck), potassium ferrocyanide (Sigma-Aldrich), potassium ferricyanide (Sigma-Aldrich), potassium bicarbonate (Sigma-Aldrich), amphotericin (Merck), miltefosine (Merck), ascorbic acid (Merck), multi-walled carbon nanotubes (Sigma-Aldrich), nitric acid (Sigma-Aldrich), sulphuric acid, (Sigma-Aldrich), ethylenediamine (Sigma Aldrich), and sodium nitrite (Merck). All chemicals used were of analytical grade.

Instrumentation

Fourier transform infrared spectroscopy (Bruker® Alpha-PATR-FT-IR, Germany) was utilised to study the functional groups on the amino functionalised multi-walled carbon nanotubes. This was followed by the use of field emission scanning electron microscopy (FE-SEM) (ZEISS, ultra plus, Germany) to study the morphology of the amino functionalised multi-walled carbon nanotubes. Energy dispersive X-ray spectroscopy was used to determine the elemental components of the amino functionalised multi-walled carbon nanotubes. All electrochemical studies were conducted using the electrochemical workstation, CH1660E (CH instrument, USA). The setup comprised a three-electrode system of the reference electrode (Ag/AgCl), counter electrode (platinum wire), and working electrode (GCE). Figure 1 illustrates briefly the procedures used in this study.

Synthesis of NH_2 Functionalised Multi-walled Carbon Nanotubes (MWCNT-NH_2)

MWCNT-NH_2 was synthesised using Zhao et al. (2013) [18] method with some changes. Firstly, pure MWCNT was functionalised using a mixture of sulphuric acid and nitric acid to obtain MWCNT-COOH. A mixture of sulphuric acid and nitric acid in a ratio of 3:1 (60 mL and 20 mL, respectively) was added to 100 mg of MWCNT. The resulting mixture was refluxed at 80 °C for an hour. The mixture was diluted with deionised water, filtered, and dried at 60 °C in an oven overnight. Afterwards, 40 mg of the MWCNT-COOH was mixed with 116 mg of $NaNO_3$ and 0.4 mL of ethylenediamine. Under stirring conditions, the mixture was heated at 60 °C for an hour. The mixture was cooled to room temperature, and then DMF was added and filtered. DMF was added to the residue from the filtration, sonicated, and filtered again. The process was repeated until a colourless mixture was obtained. The residue collected was dried overnight at 60 °C in an oven.

Formation of Complex with Miltefosine

The complex of miltefosine and MWCNT-NH_2 was formed by dissolving 5 mg of miltefosine and 5 mg of MWCNT-NH_2 in 5 mL of ethanol. The resulting mixture was sonicated for 5 min, and the solvent was evaporated using a rotary evaporator. The resulting paste was dried on a high vacuum for 24 h.

Preparation of MWCNT-NH_2 Electrode (MWCNT-NH_2/GCE)

A slurry of alumina (0.05 μM) was dispersed on the cleaning pad and used to polish the glassy carbon electrode. The electrode was then washed with deionised water to remove adsorbed particles from the surface of the electrode. This was followed by the preparation of 1 mg/mL of Mil-MWCNT-NH2 suspension. Five microlitres of the suspension was then pipetted and drop-cast onto the surface of a

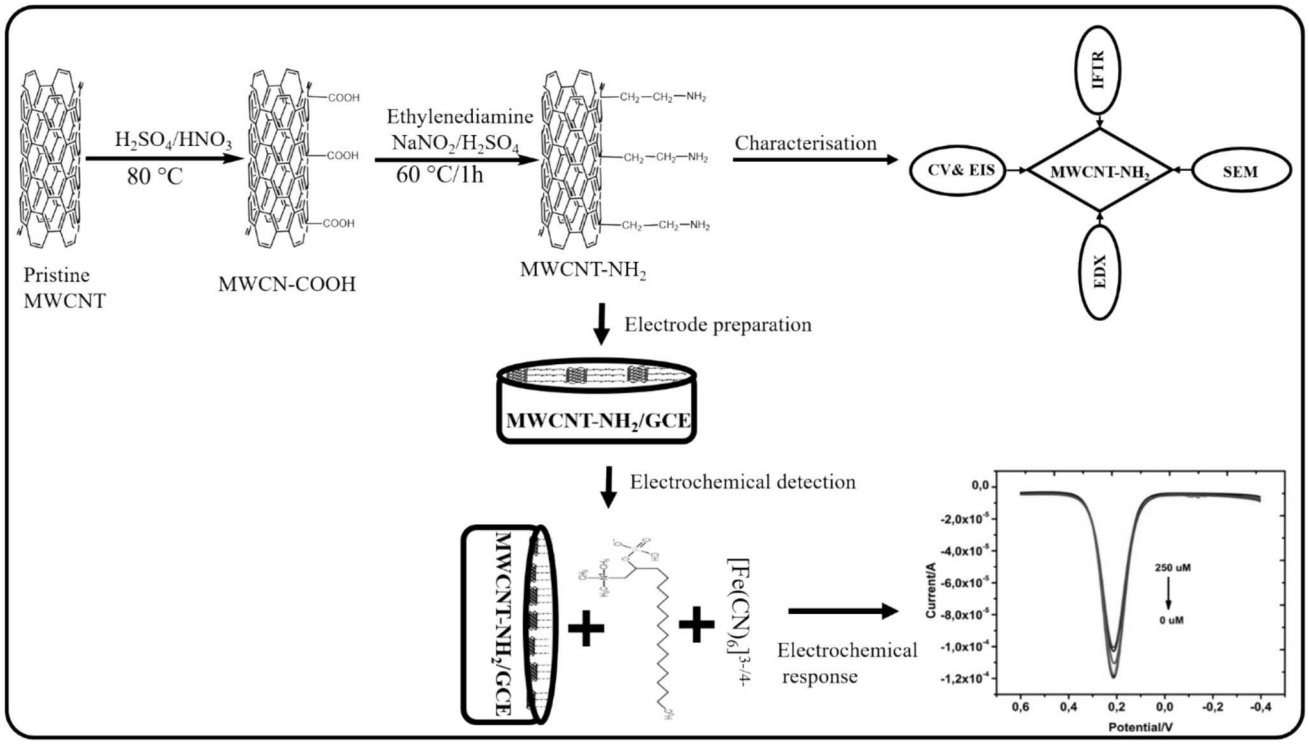

Fig. 1 Graphical summary of procedure used in this study

dry and clean electrode. Afterwards, the electrode was dried under an IR lamp.

Preparation of Urine Sample

The practical application of the MWCNT-NH_2-based sensor was assessed by detecting miltefosine in a human urine sample. The urine sample collected from a healthy person was diluted ten times to minimise the matrix effect. The diluted urine samples were spiked with miltefosine at varying concentrations (10 µM, 50 µM, 100 µM, 200 µM, and 250 µM). To each of the miltefosine-spiked diluted urine samples, 1 mg of MWCNT-NH_2 was added. The MWCNT-NH_2-modified electrode was used to detect the miltefosine spiked urine sample with $[Fe(CN)_6]^{3/4}$ as a redox couple.

Results and Discussion

Spectral Studies

SEM and EDX Studies

The surface morphology of pristine MWCNTs and MWCNT-NH_2 were studied using SEM imaging. As illustrated in Fig. 2A, the image of pristine MWCNTs showed long tubes crossing each other with little entanglement. Compared with the images of the pristine MWCNTs, the image of MWCNT-NH_2 (Fig. 2B) showed short tubes with a cluster of particles, which can be associated with the functionalisation of MWCNTs with amino groups.

To further prove the functionalisation of MWCNTs with NH_2 groups, EDX spectroscopy was used to study the elemental composition of pristine MWCNTs and MWCNTs-NH_2. As presented in Fig. 2C, the EDX spectra of MWCNTs show C (96.06%) and O (3.94%) as the constituents of MWCNTs. The EDX spectra, as presented in Fig. 2D, show that MWCNTs-NH_2 consists of C (36.54%), N (13.95%), O (29.78%), Na (6.92%), and S (12.81%). The presence of Na and S are traces from $NaNO_3$ and H_2SO_4 used in the functionalisation of MWCNTs with NH_2 groups.

FT-IR Studies

The FT-IR spectra of pristine MWCNTs, MWCNT-COOH, and MWCNT-NH_2 are presented in Fig. 3. The FT-IR spectra of the pristine MWCNTs (Fig. 3A) showed peaks at 1556 cm^{-1} and 2990.5 cm^{-1} associated with C = C stretching and C–H stretching, respectively. Compared with the MWCNTs, the spectra of MWCNT-COOH (Fig. 3B) showed new peaks at 1290 cm^{-1}, 1615 cm^{-1}, 1709.7 cm^{-1}, 2761 cm^{-1}, and 2927 cm^{-1} ascribed to C–O stretching, C = C stretching, C = O stretching, O–H stretching, and C–H stretching, respectively. Identifying these functional groups on the

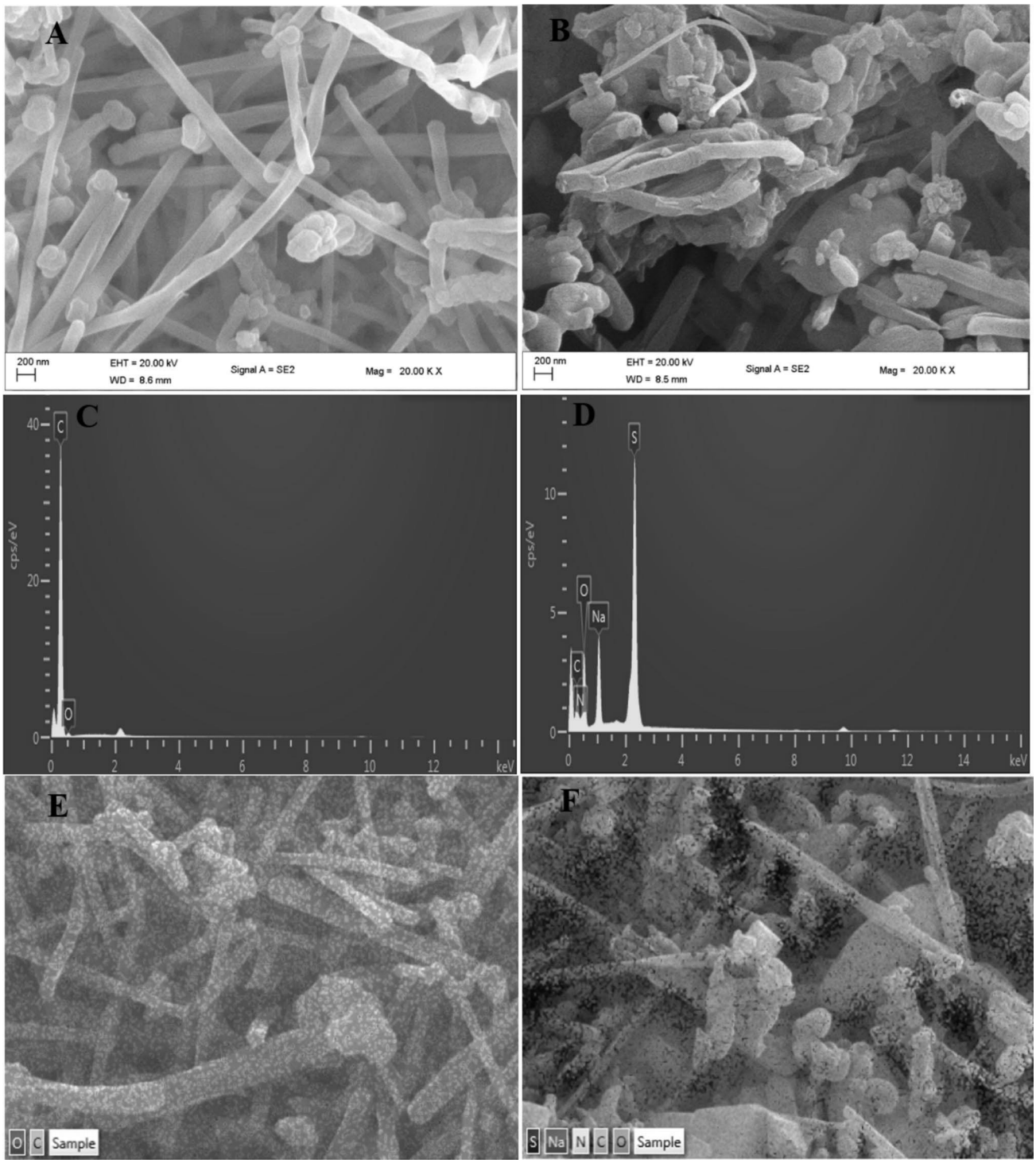

Fig. 2 **A** SEM image of MWCNTs, **B** SEM image of MWCNT-NH_2, **C** EDX spectra mapping of MWCNTs, **D** EDX spectra mapping of MWCNT-NH_2, **E** EDX spectra of MWCNTs, and **F** EDX spectra of MWCNT-NH_2

MWCNT-COOH spectra suggests that carboxylic groups were successfully attached to the MWCNTs. After confirming the functionalisation of MWCNT with COOH groups, FTIR analysis was carried out on the MWCNT-NH_2 sample. As presented in Fig. 3C, peaks were observed at 1342 cm^{-1}, 1534 cm^{-1}, 1620 cm^{-1}, and 2825 cm^{-1}. These peaks were attributed to C–N bond stretching, C = C stretching, N–H bend, and C–H stretching, respectively. The identification of peaks attributed to C–N bond stretching and N–H bend indicates that the attachment of NH_2 groups to the carboxylic

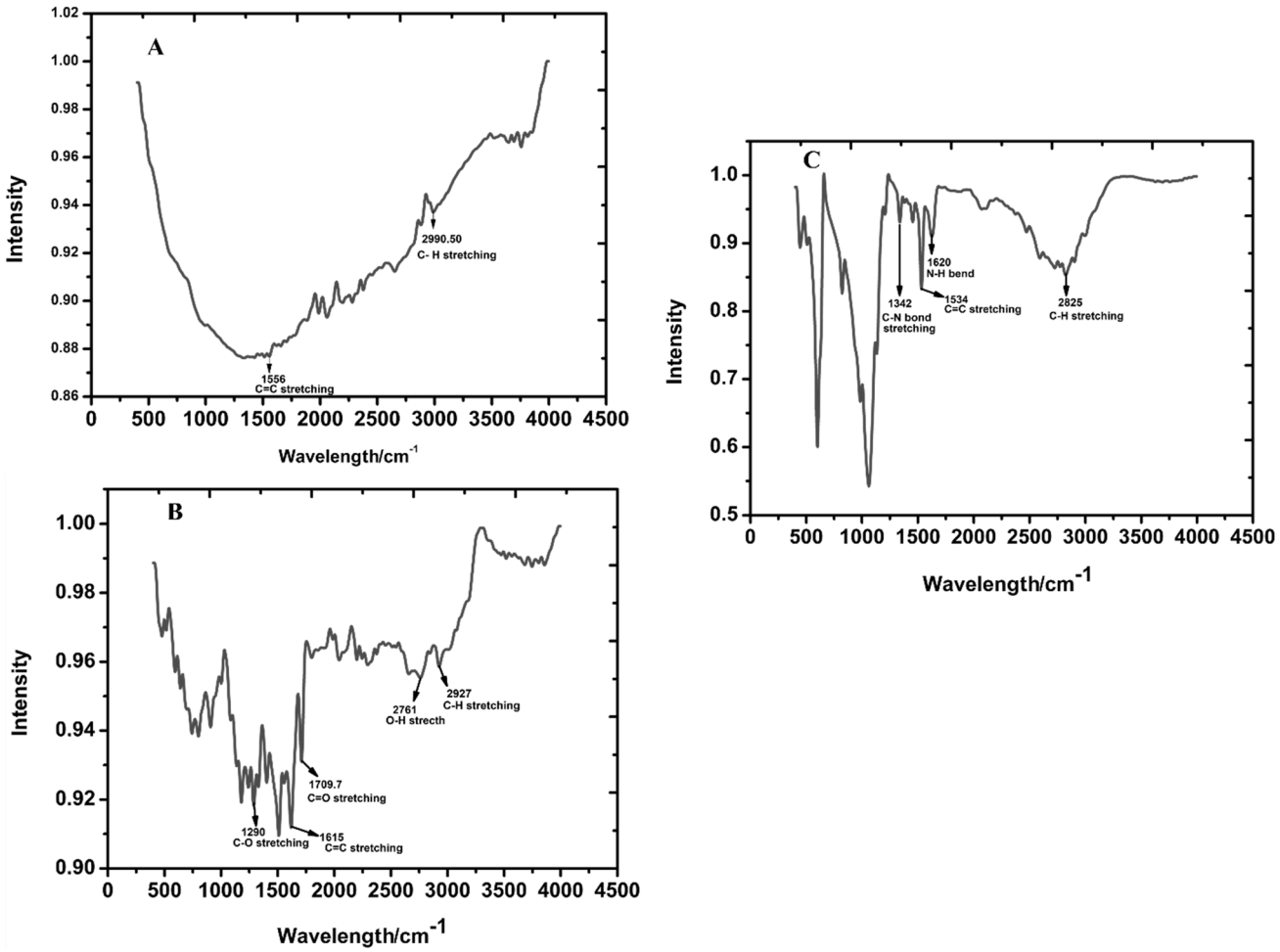

Fig. 3 FT-IR spectra of **A** pristine MWCNT, **B** MWCNT-COOH, and **C** MWCNT-NH_2

functionalised MWCNTs was successful. This analysis corroborates the SEM and EDX analysis, which confirms the successful functionalisation of MWCNTs with NH_2 groups.

Electrochemical Characterisation

The electrocatalytic properties of the synthesised NH_2 functionalised multi-walled carbon nanotubes were studied using electrochemical impedance spectroscopy (EIS) and cyclic voltammetry (CV). The interfacial electron transfer rate at the surface of the electrodes was investigated using EIS. EIS technique measures the resistance to electron transfer. EIS studies apply a low AC voltage to the system, and the resultant current is analysed. The data obtained from EIS studies is represented using the standard Randles equivalent circuit, which comprises Warburg impedance (W), charge transfer resistance (R_{ct}), resistance of the solution (R_s), and the double layer capacitance (C_{dl}) [19]. As synopsised in Table 1, R_{ct} values of 294.8 Ω and 0.001 Ω were obtained accordingly for bare GCE and MWCNT-NH_2/GCE. A low R_{ct} indicates high impedance. Furthermore, the Nyquist plot used to represent EIS is a plot of actual resistance (Z') against imaginary resistance (Z'') obtained from the standard Randles equivalent circuit. Figure 4B illustrates that the bare GCE has a big semi-circle compared to the MWCNT-NH_2/GCE, which had no visible semi-circle. This confirms that the R_{ct} values obtained as the impedance measure are directly proportional to the size of the semi-circle in the Nyquist plot. This suggests that modifying the electrode

Table 1 Parts of Randles equivalent circuit for bare GCE and MWCNT-NH_2/GCE

Parts of circuit	Bare GCE	MWCNT-NH_2/GCE
R_s/Ω	99.45	98.27
R_{ct}/Ω	294.8	0.001
W/Fg^{c-1}	7.34×10^{-4}	1.39×10^{-5}
C_{dl}/Ω$s^{-1/2}$	1.488×10^{-6}	1.326×10^{-6}

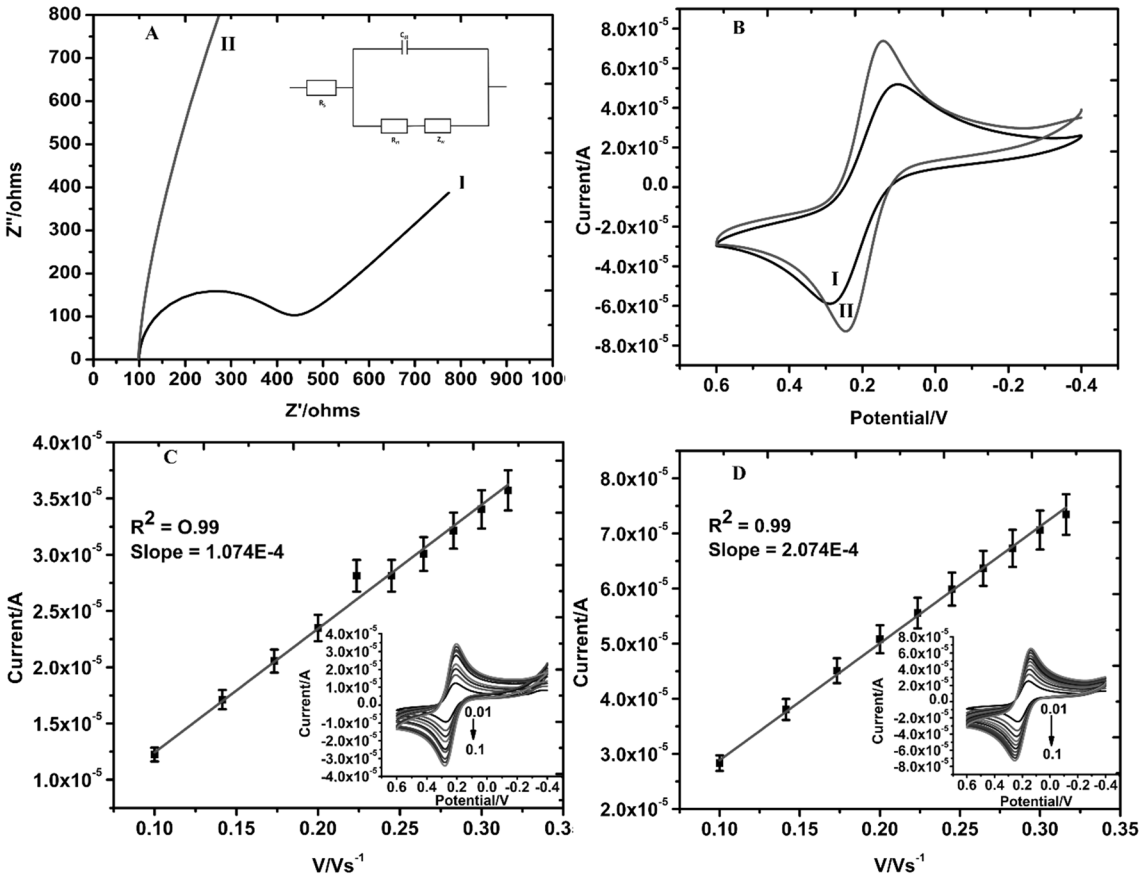

Fig. 4 **A** Cyclic voltammogram of (I) bare GCE and (II) MWCNT-NH_2, **B** EIS plot of (I) bare GCE, and (II) MWCNT-NH_2 with Randles equivalent circuit in-set, **C** linear plot of the square root of scan rate against current for bare GCE with cyclic voltammogram in-set, and **D** linear plot of the square root of scan rate against current for MWCNT-NH_2 with cyclic voltammogram in-set

with MWCNT-NH_2 improved the diffusion of electrons towards the electrode.

Cyclic voltammetry, a technique that measures the current between the working and counter electrodes as a function of the applied potential [20], was used to study the redox behaviour of the modified electrode, as presented in Fig. 4A. This study used a three-electrode system in 2.5 mM $[Fe(CN)_6]^{-3/-4}$ containing 1 M KCl. Potential varied from − 0.4 to 0.6 V was applied to the working electrode, and the resulting current was measured. Peak current of 5.635×10^{-5} A and 7.861×10^{-5} A were obtained for bare GCE and MWCNT-NH_2/GCE, respectively (Table 2). The result shows an increase in peak current from the bare GCE to the MWCNT-NH_2/GCE. This indicates that modifying the electrode with MWCNT-NH_2 nanomaterial enhanced its electron conductivity. This finding confirms the results obtained from the EIS analysis.

Determination of the Effective Surface Area of the MWCNT-NH_2 Electrode

The CV response derived from the effect of the scan rate study was employed to determine the effective electrochemical surface area of bare GCE and MWCNT-NH_2/GCE. The study involved the use of a scan rate varied from 0.01 to 0.1 V. As depicted in Fig. 4C and D, a linear graph was

Table 2 Data on the CV and effective electrochemical surface area

Electrode	CV (anodic current/A)	CV (cathodic current/A)	Effective surface area/cm^2
Bare GCE	5.635×10^{-5}	5.167×10^{-5}	0.0579
MWCNT-NH_2/GCE	7.861×10^{-5}	7.819×10^{-5}	0.1119

established between the square root of scan rate against anodic peak current. Using the Randles–Sevcik equation, the gradient obtained from the linear graph was used to calculate the effective electrochemical scan rate. The Randles–Sevcik equation used has been expressed in Eq. 1:

$$I_p = 2.69 \times 10^5 AD \frac{1}{2n} \frac{3}{2V} \frac{1}{2C_o} \quad (1)$$

where *I*p—peak current (A), *A*—surface area of electrode (cm^2), *n*—number of electrons transferred (for $K_3[Fe(CN)_6]$, $N = 1$), *D*—diffusion coefficient ($7.60 \times 10 - 6$ cm^2/s for $K_3[Fe(CN)_6]$), *V*—scan rate (V/s), and Co—concentration (mol/cm^3). As illustrated in Table 2, an effective surface area of 0.0579 cm^2 and 0.1119 cm^2 was calculated for bare GCE and MWCNT-NH_2/GCE, respectively. This observation shows that modification of the electrode with MWCNT-NH_2 increased the surface area, leading to increased conductivity, which correlates with the results from EIS and CV.

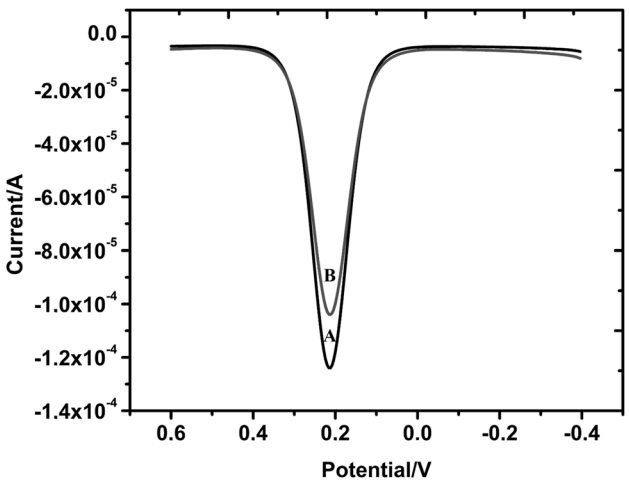

Fig. 5 Differential pulse voltammogram in 2.5 mM $[Fe(CN)_6]^{3/4}$ containing 1 M KCl at (A) MWCNT-NH_2- and (B) Mil-MWCNT-NH_2-modified electrodes

Detection Mechanism

MWCNT was functionalised with NH_2 groups to improve the solubility of MWCNTs and enhance the selectivity of material for miltefosine. According to Croft et al. [21], miltefosine interacts with receptors through the negative electrostatic surface around the phosphate groups in the structure of miltefosine. From this background, MWCNT, a highly electrocatalytic nanomaterial, was decorated with NH_2 groups to facilitate the formation of a complex between MWCNT-NH_2 and miltefosine through hydrogen bonding. Following this, a one-time shot assay of MWCNT-NH_2 was used to form a complex with miltefosine, and an observable response was produced. Using $[Fe(CN)_6]^{-3/-4}$ as a redox couple and DPV technique, the response was in the form of a reduction in peak current. Miltefosine has no electroactive centre in the structure [8]. Hence, the interaction of miltefosine with the MWCNT-NH_2-modified electrode decreases conductivity as the flow of electrons from the $[Fe(CN)_6]^{-3/-4}$ solution to the electrode is disrupted [22].

Performance of Sensor

Differential pulse voltammograms of MWCNT-NH_2 and miltefosine-spiked MWCNT-NH_2 (Mil-MWCNT-NH_2) were recorded to assess the sensor's performance. The differential pulse voltammetric studies were performed in a 2.5 mM $[Fe(CN)_6]^{-3/-4}$ containing 1 M KCl as a redox couple. As Fig. 5 illustrates, the redox peak current recorded for the Mil-MWCNT-NH_2 electrode was significantly lower than that recorded for MWCNT-NH_2. This is due to the interaction of miltefosine with the NH_2 group on the MWCNTs, disrupting the flow of electrons and reducing the redox peak current.

To establish the concentration range of the MWCNT-NH_2-based sensor, different concentrations of miltefosine (0–250 µM) were added to 1 mg/mL solution of MWCNT-NH_2, and electrochemical measurements were taken. The differential pulse voltammetric technique was used for this study because of its high sensitivity in detecting very low concentrations compared to other techniques [23]. At a potential window of − 0.4–0.6 V, the electrochemical measurements were taken with 2.5 mM $[Fe(CN)_6]^{-3/-4}$ containing 1 M KCl as a redox couple. A redox peak was seen at 0.212 V. A decrease in peak current was detected with an increment in the concentration of miltefosine (Fig. 6). Machini et al. reported a similar occurrence in their study to evaluate miltefosine-dsDNA interaction [8]. To achieve a linear response between varying concentrations of miltefosine and peak current, a linear plot of miltefosine concentrations against peak current was established. The linear regression equation has been expressed in Eq. 2.

$$Ip(A) = -8.07942 \times 10^{-8} + 1.15522 \times 10^{-4} = [\text{Miltefosine}]; R^2 = 0.98985 \quad (2)$$

The lowest detectable concentration of miltefosine was determined to be 1 µM. With the excellent response of the technique, together with the high sensitivity, selectivity, and simplicity, this assay shows promise of application as a quality control and monitoring of miltefosine.

Interference Study

An interference study was undertaken to determine the selectivity of the MWCNT-NH_2 assay to detect miltefosine. The study involved using 1 mM amphotericin, an

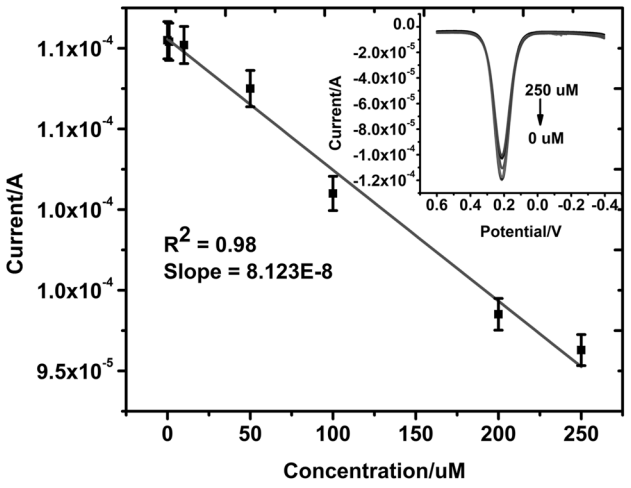

Fig. 6 Linear plot of miltefosine concentration (1–250 µM) against current with differential pulse voltammogram in-set in 2.5 mM $[Fe(CN)_6]^{3/4}$ containing 1 M KCl at a potential window of − 0.4–0.6 V

antileishmanial drug, K^+ and HCO_3^- ions, and ascorbic acid. Each of the interfering agents was incubated with 1 mg/mL of Mil-MWCNT-NH_2 for 5 min. The study involved the use of the DPV technique. As illustrated in Fig. 7, no relevant decrease in current output was observed for all the interfering agents used in this experiment. With a relative standard deviation of 0.18, the variation in the decrease in current output observed is within the 5% tolerable limit. This indicates that the MWCNT-NH_2 assay shows selectivity towards miltefosine in the presence of interfering agents.

Reproducibility Studies

To determine the reproducibility of the MWCNT-NH_2-based sensor, the assay was separately prepared and run repeatedly three times. At a potential window of − 0.4–0.6 V, the DPV technique was used, and electrochemical measurements were taken for each run. As presented in Fig. 8, the current outputs obtained were compared, and a mean of 1.21×10^{-4} was calculated. With a low relative standard deviation of 1.83, it suggests that the MWCNT-NH_2-based sensor for miltefosine detection is highly reproducible.

Real Sample Studies

Urine is one of the fluids through which miltefosine is removed from the body [9]. Also, urine is more convenient for patients who are already weak than faeces or blood samples. Owing to this, a urine sample was chosen for this study. Urine samples were collected from a healthy person and diluted ten times to reduce the matrix effect. The diluted urine was then used to prepare 1 mg/mL of MWCNT-NH_2. To aliquot of MWCNT-NH_2, varying concentrations (10–250 µM) of miltefosine were added, and electrochemical measurements were taken using the DPV technique. A linear relationship was established between varying concentrations of miltefosine and peak current, as depicted in Fig. 9. The linear regression equation represented in Eq. 3.

$$Ip(A) = -6.44774\times10^{-8} + 1.1322 \times 10^{-4} = [Miltefosine]; R^2 = 0.98144 \quad (3)$$

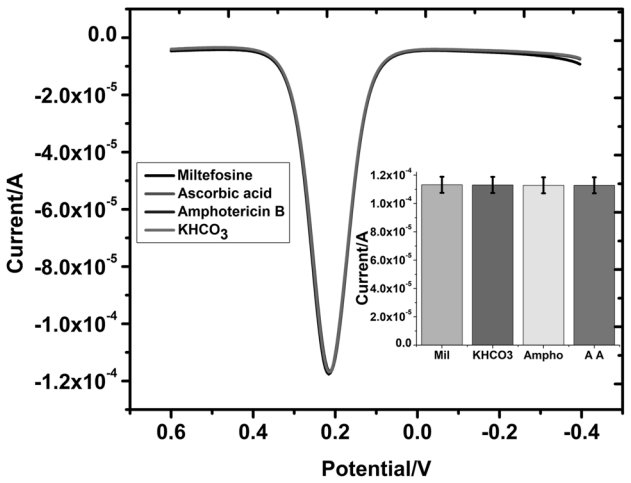

Fig. 7 Differential pulse voltammogram in 2.5 mM $[Fe(CN)_6]^{-3/-4}$ containing 1 M KCl of Mil-MWCNT-NH_2 modified electrode in the presence of amphotericin, K^+, HCO_3^-, and ascorbic acid. In-set is a column graph of interfering agents against peak current

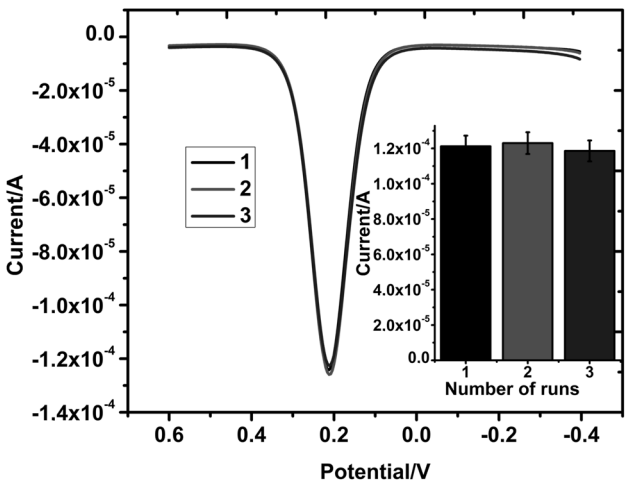

Fig. 8 Differential pulse voltammogram in 2.5 mM $[Fe(CN)_6]^{-3/-4}$ containing 1 M KCl of Mil-MWCNT-NH_2 modified electrode of reproducibility studies of three separate runs. In-set is a column graph of the number of runs against the current

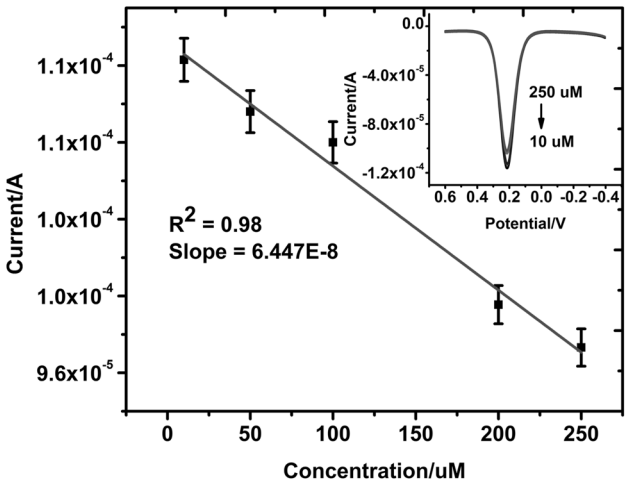

Fig. 9 Linear plot of miltefosine concentration (10–250 µM) against current with differential pulse voltammogram in-set in 2.5 mM $[Fe(CN)_6]^{3/4}$ containing 1 M KCl spiked with urine at a potential window of − 0.4–0.6 V

An increase in concentration corresponded with a decrease in peak current. A minimum detectable limit of miltefosine concentration of 1 µM was detected.

Conclusion

In summary, this study has developed, for the first time, an electrochemical sensor for detecting an antileishmanial drug, miltefosine, using $[Fe(CN)_6]^{-3/-4}$ as a redox couple. The study involved the functionalization of multi-walled carbon nanotubes with amino groups. The synthesised MWCNT-NH_2 nanomaterial was confirmed by scanning electron microscopy, energy dispersive X-ray spectroscopy, and Fourier transform infrared spectroscopy studies. The developed sensor detected miltefosine in a concentration range of 1–250 µM with a detection limit of 1 µM. Moreover, the developed sensor was shown to be reproducible and selective for miltefosine in spiked urine samples and amid interfering agents. Finally, the developed MWCNT-NH_2–based electrochemical sensor shows great potential for application in quality control of miltefosine.

Acknowledgements We sincerely thank the University of KwaZulu-Natal, the Nanotechnology for Sustainable Development platform of UKZN, and the Microscopy and Microanalysis Unit for their services and support.

Author Contribution Darko Kwabena Adu: conceptualisation, investigation, data analysis and manuscript writing. Zondi Nate: supervision and review of the manuscript. Sachin Balaso Mohite: methodology. John Alake: review of the manuscript. Blessing Wisdom Ike: review of the manuscript. Lungelo Miya: review of the manuscript. Ruchika Chauhan: supervision and review of the manuscript. Rajshekhar Karpoormath: supervision, fund, and review of the manuscript.

Funding Open access funding provided by University of KwaZulu-Natal. Rajshekhar Karpoormath was funded by the College of Health Sciences, University of KwaZulu-Natal, South Africa (grant number, RM27), for funding this study.

Data Availability All the data generated and analysed in this study have been provided in the manuscript.

Declarations

Ethical Approval The Biomedical Research Ethics Committee of the University of KwaZulu-Natal, Westville campus, granted this study an ethical exemption (00020770).

Competing Interests The authors declare no competing interests.

References

1. D.K. Adu, Z. Nate, J. Alake, B.W. Ike, M.C. Mahlalela, S.B. Mohite, S. Mokoena, R. Chauhan, R. Karpoormath, Bioelectrochemistry **157**, 108662 (2024)
2. M. P. Campos, F. B. Figueiredo, F. N. Morgado, A. R. dos S. Renzetti, S. M. M. de Souza, S. A. Pereira, R. N. Rodrigues-Da-Silva, J. D. C. Lima-Junior, and P. M. De Luca, Front Immunol **9**, 1 (2018).
3. B.R. Martins, Y.O. Barbosa, C.M.R. Andrade, L.Q. Pereira, G.F. Simão, C.J. de Oliveira, D. Correia, R.T.S. Oliveira, M.V. da Silva, A.C.A. Silva, N.O. Dantas, V. Rodrigues, R.A.A. Muñoz, R.P. Alves-Balvedi, Biosensors (Basel) **10**, 81 (2020)
4. S. Ghosh, S. Biswas, S. Mukherjee, A. Pal, A. Saxena, S. Sundar, J.-C. Dujardin, S. Das, S. Roy, R. Mukhopadhyay, B. Mukherjee, Front. Cell. Infect. Microbiol. **11**, 1 (2021)
5. R. Sivayogana, A. Krishnakumar, S. Kumaravel, R. Rajagopal, and P. Ravikanth, in *Leishmaniasis - General Aspects of a Stigmatized Disease* (IntechOpen, 2022).
6. T.P.C. Dorlo, T.A. Eggelte, P.J. de Vries, J.H. Beijnen, Analyst **137**, 1265 (2012)
7. T.P.C. Dorlo, M. Balasegaram, J.H. Beijnen, P.J. de Vries, J. Antimicrob. Chemother. **67**, 2576 (2012)
8. W.B.S. Machini, A.M. Oliveira-Brett, Electroanalysis **30**, 48 (2018)
9. S. Palić, J.H. Beijnen, T.P.C. Dorlo, Int. J. Antimicrob. Agents **59**, 106459 (2022)
10. S. Kumar, S. Tripathy, A. Jyoti, S.G. Singh, Biosens. Bioelectron. **124–125**, 205 (2019)

11. L. Díaz de León-Martínez, J. Glöckler, B. Mizaikoff, R. Flores-Ramírez, and F. Díaz-Barriga, in *Encyclopedia of Sensors and Biosensors* (Elsevier, 2023), pp. 421–440.
12. F.S. Omar, N. Duraisamy, K. Ramesh, S. Ramesh, Biosens. Bioelectron. **79**, 763 (2016)
13. F. Faridbod, V.K. Gupta, H.A. Zamani, Int. J. Electrochem. **2011**, 1 (2011)
14. M. Miyake, in *Carbon Alloys* (Elsevier, 2003), pp. 435–445.
15. E. Zagoraiou, F. Paloukis, M.K. Daletou, Nano-Structures & Nano-Objects **24**, 100566 (2020)
16. J. Alake, Z. Nate, D.K. Adu, B.W. Ike, R. Chauhan, R. Karpoormath, Electrocatalysis **14**, 232 (2023)
17. B. Deepanraj, V. Tirth, A. Algahtani, E.M. Elsehly, Alex. Eng. J. **88**, 310 (2024)
18. Z. Zhao, Z. Yang, Y. Hu, J. Li, X. Fan, Appl. Surf. Sci. **276**, 476 (2013)
19. F. Ciucci, Curr. Opin. Electrochem. **13**, 132 (2019)
20. G.A. Mabbott, J. Chem. Educ. **60**, 697 (1983)
21. S.L. Croft, J. Engel, Trans. R. Soc. Trop. Med. Hyg. **100**, S4 (2006)
22. A.A.S. Gill, S. Singh, N. Agrawal, Z. Nate, T.E. Chiwunze, N.B. Thapliyal, R. Chauhan, R. Karpoormath, Microchim. Acta **187**, 79 (2020)
23. B. J. Venton and D. J. DiScenza, in *Electrochemistry for Bioanalysis* (Elsevier, 2020), pp. 27–50.